Effects of Azimuthal Non-uniformity on the Hall Thruster Discharge

IEPC-2017-527

Presented at the 35th International Electric Propulsion Conference
Georgia Institute of Technology – Atlanta, Georgia – USA
October 8–12, 2017

Rei Kawashima[*], Junhwi Bak[†], Kimiya Komurasaki[‡], Hiroyuki Koizumi[§]
The University of Tokyo, Tokyo, 113-8656, Japan
and
Kentaro Hara[¶]
Texas A&M University, College Station, TX, 77843, USA

Abstract: An axial-azimuthal simulation of a Hall thruster using the hybrid model is conducted to investigate the effects of azimuthally non-uniform propellant feeding. In the results, azimuthally non-uniform distributions of plasma properties are captured. The trend of increasing discharge current with increasing azimuthal non-uniformity is confirmed. The azimuthal phase shift is observed between the electron density and space potential at the downstream region. This phase shift is considered to enhance the electron transport, and the reason of discharge current increase is attributed to this enhancement of electron transport.

Nomenclature

B	= magnetic flux density
i_{e}	= electron internal energy
k	= reaction rate coefficient
n_{e}	= electron number density
T_{e}	= electron temperature
u_{e}	= electron velocity
α_{B}	= Bohm diffusion coefficient
α_{E}	= energy loss coefficient
Γ_{n}	= neutral number flux density
ν	= collision frequency
μ_{e}	= electron mobility
ϕ	= space potential
Ω_{e}	= electron Hall parameter
Subscripts	
$\perp$	= cross-field
ion	= ionization
ela	= elastic

[*]Assistant Professor, Department of Aeronautics and Astronautics, 7-3-1 Hongo, Bunkyo.
[†]Graduate Student, Department of Aeronautics and Astronautics, 7-3-1 Hongo, Bunkyo.
[‡]Professor, Department of Aeronautics and Astronautics, 7-3-1 Hongo, Bunkyo.
[§]Associate Professor, Department of Advanced Energy, 5-1-5 Kashiwanoha, Kashiwa.
[¶]Assistant Professor, Department of Aerospace Engineering, H.R. Bright Building.

I. Introduction

Hall thruster is a promising candidate of high-power electric propulsion system which enables next-generation missions such as the manned Mars mission and solar power satellite. In Japan, a collaborative research has been initiated to develop a 5 kW class thruster with anode layer (TAL).[1] In the development of the TAL, one of the important issues is how to reduce the discharge current oscillation.

One proposed method to reduce the discharge oscillation is the addition of azimuthal non-uniformity. Figure 1 shows the operation of a 0.6 kW-level TAL with the azimuthally non-uniform propellant supply.[2] It has been reported that the azimuthal non-uniform propellant feeding is effective in mitigating the discharge oscillation. However, it has also been reported that the discharge current is increased, and eventually the thruster performance is degraded. To attain the balance between the low discharge oscillation and high thruster performance, the, a further investigation on the effects of azimuthal non-uniformity is required.

The objective of this research is the numerical analysis on the effects of azimuthal non-uniformity in the Hall thruster discharge. An axial-azimuthal two-dimensional simulation based on the particle-fluid hybrid model is conducted. As the method to introduce the azimuthal non-uniformity, non-uniform propellant feeding is treated in this paper.

II. Axial-azimuthal Two-dimensional Hybrid Model

II.A. Electron basic equations

The fundamental equations for electron fluid are the two-dimensional electron mass and momentum conservation equations in quasi-neutral plasmas, and one-dimensional energy conservation equation. In the mass conservation equation, the electron number density is treated as a time-constant distribution by assuming the quasi-neutrality. Thus, the mass conservation equation is regarded as the equation of continuity as follows:

$$\nabla \cdot (n_{\mathrm{e}} \vec{u}_{\mathrm{e}}) = n_{\mathrm{e}} \nu_{\mathrm{ion}}. \tag{1}$$

Conservation of the electron momentum is derived by assuming inertialess electrons, as follows:

$$-n_{\mathrm{e}} [\mu] \nabla \phi + [\mu] \nabla (n_{\mathrm{e}} T_{\mathrm{e}}) = -n_{\mathrm{e}} \vec{u}_{\mathrm{e}}, \tag{2}$$

where the electron mobility tensor $[\mu]$ is given as follows:

$$[\mu] = \mu_{\mathrm{e},\perp} \begin{bmatrix} 1 & \Omega_{\mathrm{e}} \\ -\Omega_{\mathrm{e}} & 1 \end{bmatrix}. \tag{3}$$

Electron temperature is assumed to be axisymmetric, owing to the large electron mobility in the azimuthal direction. Hence, the energy conservation equation is calculated only in the axial direction. In the energy conservation equation, the kinetic energy is neglected, and the conservation of electron internal energy is considered. The energy conservation equation is written as follows:

$$\frac{\partial}{\partial t}\left(\frac{3}{2} e n_{\mathrm{e}} T_{\mathrm{e}}\right) + \frac{\partial}{\partial x}\left(\frac{5}{2} e n_{\mathrm{e}} T_{\mathrm{e}} u_{\mathrm{e}} - \frac{5}{2} e n_{\mathrm{e}} T_{\mathrm{e}} \mu_{\mathrm{e},\perp} \frac{\partial T_{\mathrm{e}}}{\partial x}\right) = e n_{\mathrm{e}} u_{\mathrm{e}} \frac{\partial \phi}{\partial x} - \alpha_{\mathrm{E}} e \varepsilon_{\mathrm{ion}} n_{\mathrm{e}} \nu_{\mathrm{ion}}. \tag{4}$$

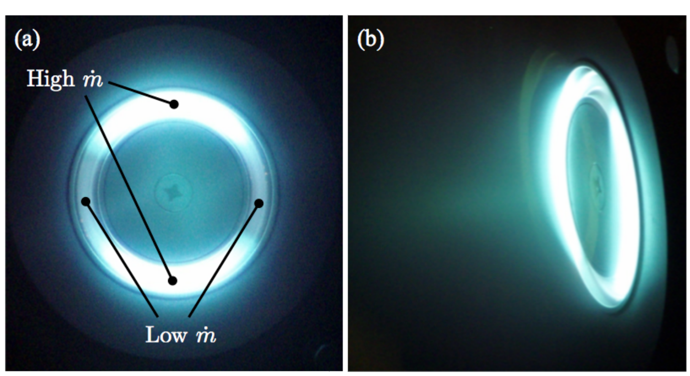

Figure 1. Thruster operation with azimuthal non-uniform propellant supply. (a) front view, and (b) side view.

where $\alpha_{\rm E}$ is the coefficient to handle the energy losses of ionization, excitation, and radiation with single term. This coefficient is experimentally determined as a function of electron temperature.[3] It is noted that the energy losses to the channel walls are assumed to be negligibly small.

II.B. Electron mobility

In the previous numerical works of axial-azimuthal hybrid simulations, the classical electron mobility was used.[4,5] However, according to the recent particle simulations which reproduced the empirical anomalous electron transport, the wavelength of the fluctuation in the azimuthal direction may be in mm-order.[6,7] Because the present simulation handles the full cylinder of the Hall thruster discharge channel, it is difficult to resolve the fluctuations in mm-order. Hence an anomalous electron transport model is needed.

A lot of models have been proposed for accurate expression of the mobility in the perpendicular direction of magnetic lines of force. The most standard model may be to include both of the classical and anomalous diffusions as follows:

$$\mu_{\rm e,\perp} = \mu_{\rm e,cla} + \mu_{\rm e,B} = \frac{\mu_{\rm e}}{1+\Omega_{\rm e}^2} + \frac{\alpha_{\rm B}}{16B}. \tag{5}$$

where $\alpha_{\rm B}$ is the Bohm diffusion coefficient. Referring the previous studies about the $\alpha_{\rm B}$,[8] the axial distribution of $\alpha_{\rm B}$ is determined as shown in Fig. 2(a). A representative example of axial distribution of cross-field electron mobility is presented in Fig. 2(b).

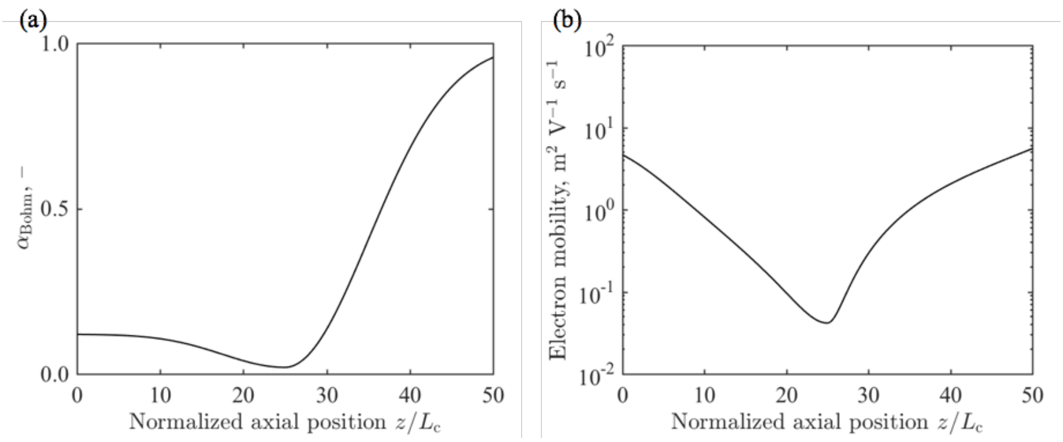

Figure 2. Axial distribution of (a) Bohm coefficient $\alpha_{\rm B}$, and (b) anomalous electron mobility.

III. Numerical Method and Calculation Condition

III.A. Ions and Neutral Particles

The ionization collision frequency and total collision frequency are calculated by using the collisional reaction rate coefficients.[9] It is noted that only first-ionization of xenon is treated in this calculation. Inter-particle collisions are neglected in the present simulation. To simplify the calculation, the effect of ion magnetization is neglected.

The advancement of each particle is implemented by the leap-frog method, which produces a second-order time accuracy. A first-order particle weighting, or cloud-in-cell model[10] is used for the weighting function in the PIC method. The time step interval is set as $\Delta t \sim 1.0 \times 10^{-8}$ s. The number of macro particles is adjusted to make each cell contains $\sim$ 200 macro particles averagely, and usually $\sim 10^5$ macro particles flow in the calculation region.

III.B. Electron Mass and Momentum Equations

In conventional approaches, Eq. (1) and Eq. (2) are integrated into an elliptic equation to solve for the space potential.[11] It has been reported that there is a numerical instability in the potential solver for the axial-azimuthal coordinate.[5] In the electron mobility tensor in Eq. (5), the non-diagonal elements can be significant compared to diagonal elements, since $\Omega_e \gg 1$ in Hall thrusters. In this case, this equation becomes an anisotropic diffusion equation, and it is difficult to maintain a stability while computing this equation because the cross-diffusion terms cause failure of the diagonal dominance of the coefficient matrix.[12]

Alternatively, the hyperbolic-equation system approach using pseudo-time advancement terms is considered. This approach has been developed for robust computation of magnetized electron fluids. The processes for deriving the hyperbolic system were presented elsewhere.[13,14] In the sub-loop for the electron mass and momentum equations, the calculation must be continued until a steady-state is reached, since these equations are handled as time-independent equations. In the hyperbolic system approach, a preconditioning technique is effective to avoid the numerical stiffness and accelerate the convergence. Here, Eq. (2) is converted as follows:

$$-en_e\nabla\phi + \nabla\left(en_eT_e\right) = -m_e\nu_{ela}\begin{bmatrix} 1 & -\Omega_e \\ \Omega_e & 1 \end{bmatrix} n_e\vec{u}_e, \tag{6}$$

Pseudo-time advance terms of electron momentum are introduced to Eq. (6). This preconditioning method is quite simple, but it is supposed to be effective in avoiding the issue of numerical stiffness in the hyperbolic system approach. In the present simulation, a second-order upwind method using the total variation diminishing monotonic upwind scheme for conservation laws (TVD-MUSCL) technique with the minmod limiter function, is used for space discretization. Concerning the time integration, an implicit method based on the alternating-direction-implicit symmetric Gauss-Seidel (ADI-SGS) method[15] is implemented.

III.C. Electron Energy Equation

The electron energy equation is calculated only in the axial direction, and electron temperature is assumed to be symmetric in the azimuthal direction. Two-dimensional plasma properties such as the ion density and neutral density are averaged in the azimuthal direction to produce axial distributions. These axial distributions are used in the calculation of electron energy equation. Electron internal energy i_e is selected as the variable for the electron energy equation, and Eq. (4) is rewritten as follows:

$$\frac{\partial i_e}{\partial t} + \frac{\partial}{\partial x}\left(Ci_e - Di_e\right) = S, \tag{7}$$

where

$$C = \frac{5}{3}\left(u_e + \mu_{e,\perp}T_e\frac{\partial}{\partial x}\left(\ln n_e\right)\right), \qquad D = \frac{5}{3}\mu_{e,\perp}T_e, \qquad S = en_eu_e\frac{\partial\phi}{\partial x} - \alpha e\varepsilon_{ion}n_e\nu_{ion}. \tag{8}$$

Eq. (7) is regarded as a standard advection-diffusion equation. The advection term is discretized by using a second-order upwind method. The diffusion term is discretized by using a second-order central differencing. The time integration is implemented by using a first-order fully implicit method incorporated with the direct matrix inversion method. The electron energy equation is handled as time-dependent, and the time step is typically set as 1.0×10^{-9} s.

III.D. Calculation Condition

In this study, an SPT-100 like Hall thruster is assumed as the calculation target. The input parameters are presented in Table 1 and the calculation region is illustrated in Fig. 3(a). A 48 × 48 rectangular mesh is used in the computation, for both of the PIC and electron fluid calculations. Fig. 3(b) shows the assumed axial distribution of magnetic flux density. The peak magnetic flux density B_p is set as 17.5 mT in this paper.

To simulate the condition of azimuthal non-uniform propellant feeding, the neutral injection rate from the anode is controlled. In this simulation, a sinusoidal distribution of anode neutral flux $\Gamma_{n,anode}$ is assumed as follows:

$$\Gamma_n = \Gamma_{n,ave}\left(1 - \frac{\Gamma_{n,dif}}{\Gamma_{n,ave}}\cos\left(\frac{2\pi N}{L_y}y\right)\right), \qquad 0 \le \frac{\Gamma_{n,dif}}{\Gamma_{n,ave}} \le 1, \tag{9}$$

where $\Gamma_{n,ave}$ is the average neutral flux density. $\Gamma_{n,dif}/\Gamma_{n,ave}$ is the differential neutral flow ratio, and if this ratio is large, a strong non-uniform propellant feeding is achieved. The integer number N determines the number of neutral flow ports for high and low mass flow rates. In this simulation, N is selected as 2 to reproduce the situation in Fig. 1.

Table 1. The input parameters assumed in the simulation.

Parameter	Value
Mass flow rate	5.0 mg/s
Discharge voltage	300 V
Channel centerline diameter	80 mm
Channel width	15 mm
Anode temperature	850 K

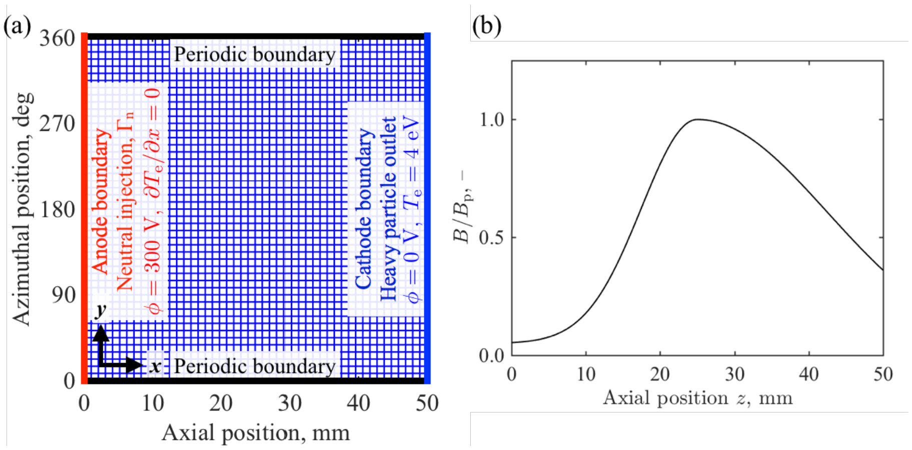

Figure 3. (a) Calculation region and 48 × 48 computational mesh. (b) Axial distribution of radial magnetic flux density.

IV. Results and Discussion

IV.A. Axial 1D Simulation Results of Uniform Supply Case

In advance of the axial-azimuthal 2D simulation, an axial 1D hybrid PIC simulation has been conducted. The purpose of this simulation is to verify that the electron mobility model in the present model yields reasonable distributions of plasma properties. The condition of uniform propellant supply is simulated.

The simulated axial distributions of plasma properties are shown in Fig. 4. The peak ion density is $\sim 1.0 \times 10^{19}$ m^{-3}. This value is approximately one-order higher than the typical simulated ion density in the axial-radial simulation of SPT-100.[16] The large ion density is attributed to the assumption of no ion loss to the channel walls. The peak electron temperature is ~ 60 eV, and this value is also large compared with the previous simulations of SPT-100. The reason of the high electron temperature is also associated with the zero electron energy loss to the channel walls.

The simulation is successfully continued for 5 ms despite the existence of breathing oscillation. The distributions of space potential and electron temperature are considered to be reasonable. Hence the electron mobility model is supposed to be useful for the numerical experiments of non-uniform propellant supply cases.

IV.B. Axial-azimuthal 2D Simulation of Non-uniform Supply

Axial-azimuthal 2D simulations are conducted for non-uniform propellant supply cases. The inflow neutral flux is controlled by setting N of 2 and $\Gamma_{\rm n,dif}/\Gamma_{\rm n,ave}$ of 0.0 to 1.0 with the interval of 0.2. The distributions of electron number density and space potential for the cases of $\Gamma_{\rm n,dif}/\Gamma_{\rm n,ave}$ of 0.0, 0.6, and 1.0 are shown in Fig. 5.

In the electron number density distributions, the azimuthal non-uniformity becomes stronger as the differential neutral flow ratio is increased. The peak of electron density exists at azimuthal position of 90 and 270 deg, which correspond to the region of high neutral inflow fluxes. The space potential distribution also becomes non-uniform in the azimuthal direction in the cases of non-uniform propellant supply. High space potential regions are observed at around the regions of high electron density. It is considered that

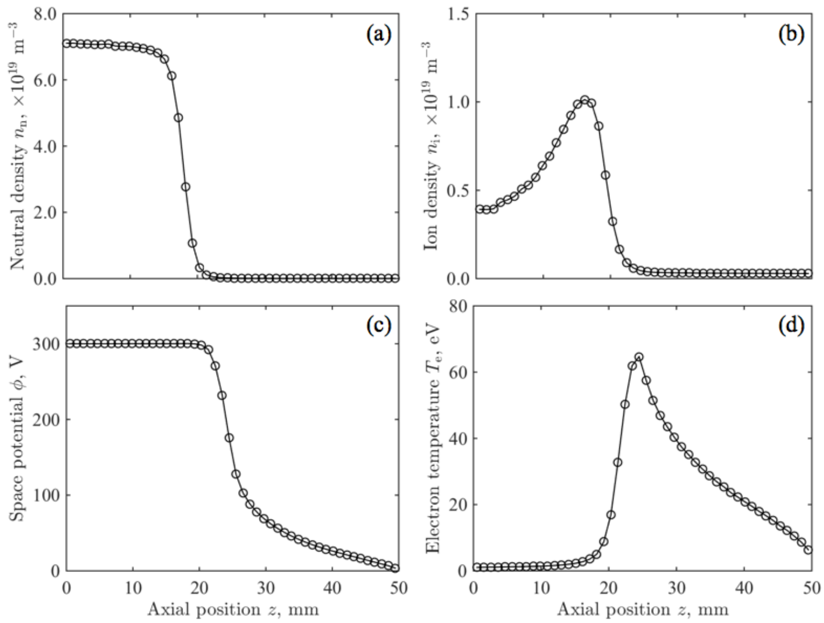

Figure 4. Time-averaged axial distribution of plasma properties in the case of uniform propellant supply ($\Gamma_{\mathrm{n,dif}}/\Gamma_{\mathrm{n,ave}} = 0.0$) simulated by the axial 1D hybrid PIC code. (a) neutral number density n_n, (b) ion number density n_i, (c) space potential ϕ, and (d) electron temperature T_e

these high potential regions are formed by the mechanism of ambipolar diffusion. The electron streamline distribution becomes complicated when the non-uniform supply is applied. As shown in Fig. 5(a2), in the case of uniform supply, the electrons basically move in the azimuthal direction, and they gradually approach the anode. However, in the cases of non-uniform supply, the electrons move downstream and upstream, with rotating in the azimuthal direction. This electron motion is supposed to reflect the direction of $E \times B$. It is concluded that the present model captures the plasma properties non-uniform in the azimuthal direction and complicated electron streamlines, when the azimuthal non-uniformity is introduced.

The trends of discharge current and ion beam current are examined when the azimuthally non-uniform propellant supply is applied. Figure 6 shows the discharge current ion beam current for various $\Gamma_{\mathrm{n,dif}}/\Gamma_{\mathrm{n,ave}}$ values, normalized by the $\Gamma_{\mathrm{n,dif}}/\Gamma_{\mathrm{n,ave}} = 0.0$ case values. The discharge current gradually increases as the differential neutral flow rate becomes larger. On the other hand, the ion beam current remains almost constant. This tendency is consistent with the experimental results.[2] The present model reproduces the trend of increasing discharge current with maintained ion beam current when the azimuthal non-uniformity becomes stronger.

The reason of increasing discharge current is further investigated. In the non-uniform supply cases, the azimuthal electric field E_θ is generated. Thus, the axial electron flux induced by $E_\theta \times B_r$ is supposed to play an important role. The azimuthal distributions of electron number density and space potential of $\Gamma_{\mathrm{n,dif}}/\Gamma_{\mathrm{n,ave}} = 1.0$ case is shown in Fig. 7. As shown in Fig. 7(a), at the location of peak electron density at $z = 16$ mm, the azimuthal phases are almost matched between the electron number density and space potential. In this case, the same amount of electron fluxes are induced to the upstream and downstream directions, and hence they are cancelled out. However, at the downstream region at $z = 40$ mm, the phase shift is observed between the electron number density and space potential. The high electron density regions exist in the regions of $90^\circ < \theta < 135^\circ$ and $270^\circ < \theta < 315^\circ$, and at that region, $+E_\theta$ is generated. On the other hand, at the low electron density regions, $-E_\theta$ is generated. Therefore, the electron flux flowing to the upstream direction is increased as a net current. It is considered that the azimuthal non-uniform propellant supply enhances the electron transport at the downstream region. This enhancement is the reason for the discharge current increase in the cases of non-uniform propellant supply.

The phase shift between the electron density and space potential has also been observed in the numerical analyses of turbulent-induced anomalous electron transport and rotating spokes.[6,17] The research about the similarity between the artificial azimuthal non-uniformity and anomalous electron transport is reserved for future study.

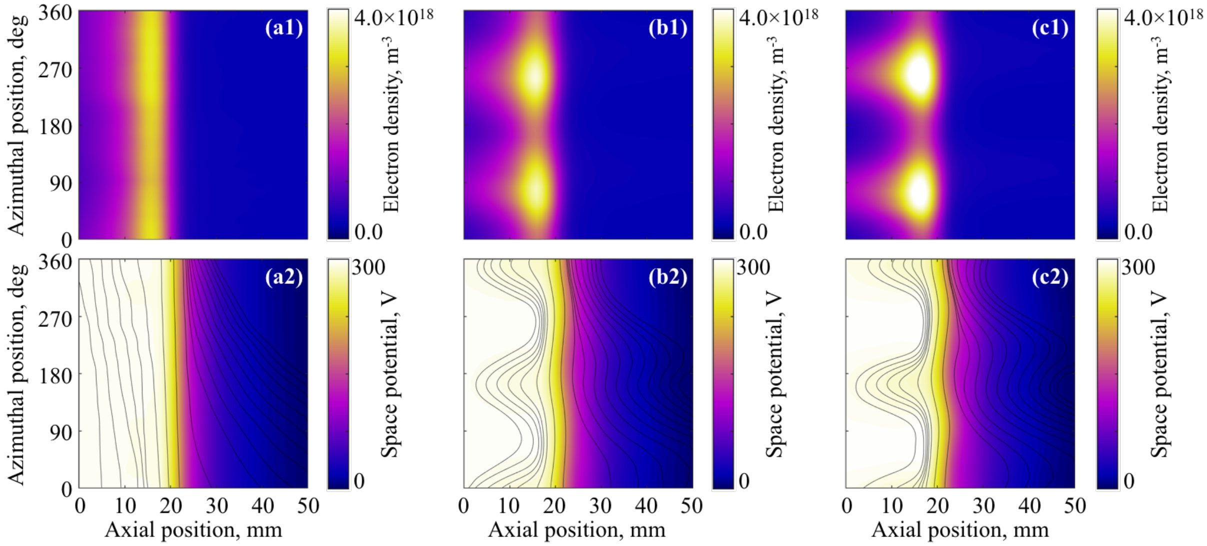

Figure 5. Time-averaged two-dimensional plasma properties in the cases of (a) $\Gamma_{\mathrm{n,dif}}/\Gamma_{\mathrm{n,ave}} = 0.0$, (b) $\Gamma_{\mathrm{n,dif}}/\Gamma_{\mathrm{n,ave}} = 0.6$, and (c) $\Gamma_{\mathrm{n,dif}}/\Gamma_{\mathrm{n,ave}} = 1.0$. (a1), (b1), and (c1) are the electron density, and (a2), (b2), and (c2) are the space potential overlaid with electron streamlines.

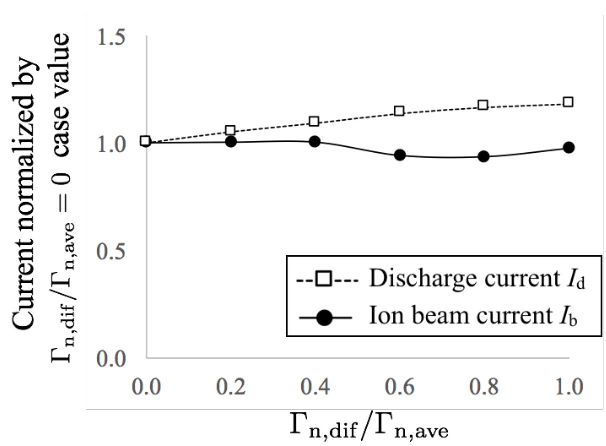

Figure 6. Simulated discharge current and ion beam current normalized by the $\Gamma_{\mathrm{n,dif}}/\Gamma_{\mathrm{n,ave}} = 0.0$ case values.

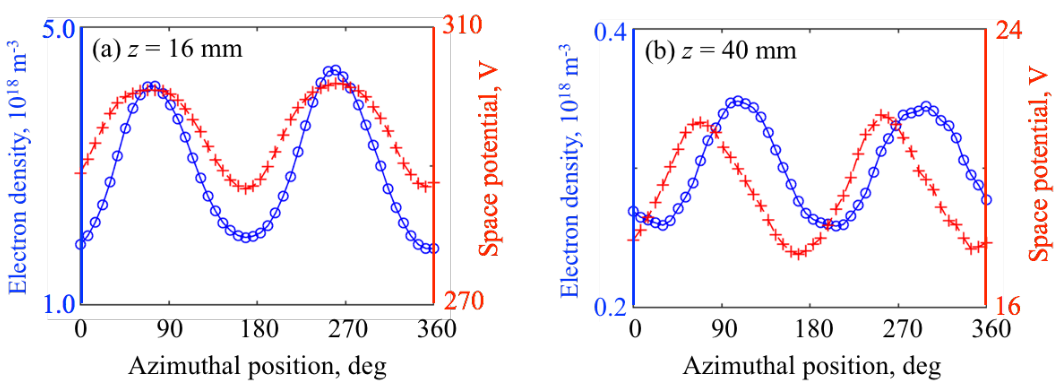

Figure 7. Azimuthal distributions of electron density and space potential at (a) $z = 16$ mm and (b) $z = 40$ mm.

V. Conclusion

The effects of azimuthal non-uniform propellant supply are investigated by using the axial-azimuthal hybrid model. In the present model, the space potential is calculated in axial-azimuthal two dimensions, whereas the electron temperature is assumed to be axisymmetric. The anomalous electron mobility is adopted and the effects of channel wall is neglected. Electron flux conservation is strictly calculated by using the hyperbolic system approach.

In the simulation results of non-uniform propellant supply cases, the azimuthally non-uniform plasma properties are successfully captured. Owing to the generation of E_θ, the electron flow behavior is complicated in the non-uniform supply cases. The trend of increasing discharge current with maintained ion beam current as the azimuthal non-uniformity becomes strong, is confirmed. Further, the reason of the discharge current increase is investigated. The azimuthal phase shift is observed between the electron number density and space potential, at the downstream region. It is considered that the azimuthal non-uniform propellant supply enhances the electron transport at the downstream region, resulting in the increment of the discharge current. This mechanism may be similar to the physics of turbulent-induced anomalous electron transport and rotating spokes. Currently, experimental measurements of plasma properties in non-uniform propellant supply cases are being conducted by using the RAIJIN66 thruster.[18] One of the future works will be to validate the model by comparing the simulation results with measurements.

References

[1]Hamada, Y., Bak, J., Kawashima, R., Koizumi, H., Komurasaki, K., Yamamoto, N., Egawa, Y., Funaki, I., Iihara, S., Cho, S., Kubota, K., Watanabe, H., Fuchigami, K., Tashiro, Y., Takahata, Y., Kakuma, T., Furukubo, Y., and Tahara, H., "Hall Thruster Development for Japanese Space Propulsion Programs," *Trans. Japan Soc. Aero. Space Sci.*, Vol. 60, No. 5, 2017, pp. 320–326.

[2]Fukushima, Y., Yokota, S., Takahashi, D., Hara, K., Cho, S., Komurasaki, K., and Arakawa, Y., "Discharge Stabilization Method of an Anode Layer Type Hall Thruster by Non-uniform Propellant Flow," 31st International Electric Propulsion Conference, IEPC-2009-148, 2009.

[3]Dugan, J. J. and Sovie, R., "Volume Ion Production Costs in Tenuous Plasmas: a General Atom Theory and Detailed Results for Helium, Argon, and Cesium," NASA Technical Note, D-4150, 1967.

[4]Lam, C., Fernandez, E., and Cappelli, M., "A 2-D Hybrid Hall Thruster Simulation That Resolves the E x B Electron Drift Direction," *Plasma Science, IEEE Transactions on Plasma Science*, Vol. 43, No. 1, 2015, pp. 86–94.

[5]Fernandez, E., Dowdy, C., and Aley, J., "Characterization of Fluctuations in Hybrid Axial-Azimuthal Hall Thruster Simulations," 34th International Electric Propulsion Conference, IEPC-2015-313, 2015.

[6]Lafleur, T., Baalrud, S. D., and Chabert, P., "Theory for the anomalous electron transport in Hall effect thrusters. I. Insights from particle-in-cell simulations," *Physics of Plasmas*, Vol. 23, No. 5, 2016, pp. 053502.

[7]Lafleur, T., Baalrud, S. D., and Chabert, P., "Theory for the anomalous electron transport in Hall effect thrusters. II. Kinetic model," *Physics of Plasmas*, Vol. 23, No. 5, 2016, pp. 053503.

[8]Hofer, R. R., Katz, I., Mikellides, I. G., Goebel, D. M., and Jameson, K. K., "Efficacy of Electron Mobility Models in Hybrid-PIC Hall Thruster Simulations," 44th Joint Propulsion Conference and Exhibit, AIAA 2008-4924, 2007.

[9]Goebel, D. M. and Katz, I., *Fundamentals of electric propulsion: ion and Hall thrusters*, Vol. 2, John Wiley and Sons, 2008.

[10]Birdsall, C. K. and Langdon, A. B., *Plasma physics via computer simulation*, CRC Press, 2004.

[11]Komurasaki, K. and Arakawa, Y., "Two-dimensional numerical model of plasma flow in a Hall thruster," *Journal of Propulsion and Power*, Vol. 11, No. 6, 1995, pp. 1317 – 1323.

[12]Kawashima, R., Komurasaki, K., and Schönherr, T., "A hyperbolic-equation system approach for magnetized electron fluids in quasi-neutral plasmas," *Journal of Computational Physics*, Vol. 284, 2015, pp. 59–69.

[13]Kawashima, R., Komurasaki, K., Schönherr, T., and Koizumi, H., "Magnetized Electron Flow Calculation Using a Hyperbolic System," 54th AIAA Aerospace Science Meeting, AIAA 2016-2159, 2016.

[14]Kawashima, R., Hara, K., Komurasaki, K., and Koizumi, H., "A Unified Model for Axial-Radial and Axial-Azimuthal Hall Thruster Simulations," 52nd Joint Propulsion Conference and Exhibit, AIAA 2016-4726, 2016.

[15]Nishida, H. and Nonomura, T., "ADI-SGS scheme on ideal magnetohydrodynamics," *Journal of Computational Physics*, Vol. 228, No. 9, 2009, pp. 3182 – 3188.

[16]Hofer, R., Mikellides, I., Katz, I., and Goebel, D., "Wall Sheath and Electron Mobility Modeling in Hybrid-PIC Hall Thruster Simulations," 43rd Joint Propulsion Conference and Exhibit, AIAA 2007-5267, 2007.

[17]Boeuf, J.-P., "Tutorial: Physics and modeling of Hall thrusters," *Journal of Applied Physics*, Vol. 121, No. 1, 2017, pp. 011101.

[18]Hamada, Y., Kawashima, R., Komurasaki, K., Yamamoto, N., Tahara, H., and Miyasaka, T., "Development Status of 5 kW Class Anode-Layer Type Hall thruster: RAIJIN94," 35th International Electric Propulsion Conference, IEPC-2017-412, 2017.